PALADYN Journal of Behavioral Robotics

VERSITA

Research Article · DOI: 10.2478/s13230-011-0006-8 · JBR · 1(4) · 2010 · 198-203

A teleoperation system for micro-invasive brain surgery

Rudy Manganelli[1], **Francesco Chinello**[1], **Alessandro Formaglio**[1*], **Domenico Prattichizzo**[1,2]

1 *Department of Information Engineering,University of Siena, Italy*

2 *Italian Institute of Technology, Genova, Italy*

Received 10 December 2010

Accepted 10 February 2011

Abstract

This paper deals with controller design issues for a neurosurgical teleoperator system. The specific application of interest consists of remotely inserting a linear-stage rigid endoscope into the patient's brain for microinvasive neurosurgery interventions. This work aims at evaluating advantages and drawbacks of using a general-purpose control architecture versus a simpler task-oriented architecture, from a point of view of stability and transparency. Experiments revealed that in spite of its simplicity, the task-oriented design allows an improvement in the trade-off between performance, transparency and stability requirements.

Keywords

teleoperation · haptics · medical robots

1. Introduction

In recent years, the usage of robotic teleoperation systems in the operation room is increasing rapidly [1]. Among the large variety of applications dealing with teleoperation, in this paper attention is directed towards microinvasive neurosurgery. The scenario is the one presented in[2] where a master-slave telemanipulation system must be designed to drive the insertion of a linear-stage rigid endoscope into the brain of the patient for neurosurgery interventions. The endoscope insertion will be assisted by a haptic interface, which will extend and complement the surgeon's skills during the insertion process. The device will be responsible for the reproduction and the eventual amplification of the forces experienced by the end-effector linear stage via a force feedback interface onto the surgeon's hand. This teleoperation architecture will enable the servo-assisted insertion of the probe into soft tissues without the loss of an eventually augmented kinesthetic perception.

Regarding transparency, the controller should be able to virtually reflect to the user the same real impedance of the operational environment, in addition to guaranteeing safety and stability as well. Several approaches can be found in the literature, in which the transparency has been quantitatively defined in different ways. In [3], the transparency has been defined as the perfect position and force matching between the master and slave manipulator. In [4], the transparency has been defined in terms of the ratio between the real and the rendered impedance. In [5], the fidelity metric is based on the ability of the system to render environmental compliance changes while taking into account some cognitive aspects of the operator perception. Although different point of views, all solutions are obviously subject to the same stability requirements, i.e. the system should not exhibit vibration or divergent behavior, under any operating conditions and for any environments. However, as discussed in detail in [4], the stability is often achieved by adding damping elements in the control loop, eventually using nonlinear or switching techniques. For example, in [6] the reflected impedance is intentionally shaped by the bilateral controller in order to improve perception by the user and to achieve robust stability. In any case, any change of the rendered impedance results in a transparency degradation. In summary, transparency and stability may be conflicting design goals for a teleoperation controller, hence a suitable trade-off must achieved to guarantee realistic and stable operation in a wide range of environment impedance and in the presence of signal latency [7–11].

In addition to providing a comparison between different control architectures available in the literature, this paper evaluates and discusses the possibility of adapting existing control schemes to the application of interest, before undertaking the development of a new specific and task-oriented control architecture. The Time-Domain Passivity Control (PC) approach introduced in [12] is considered. Then, a task-oriented proportional-derivative (PD) control is proposed. The PD control is designed taking into account the slave maximum velocity during the needle insertion which is upper bounded at 5 mm/sec. The PD controller allows filtering out all surgeon motions exceeding a given bandwidth, thus preferring task accuracy and safety with respect to dynamic performances.

Preliminary experimental results of this study were introduced in our previous contribution [13]. In this work, we improved the mathematical formalization of the two-port network model adopted for the Time-Domain Passivity Control, along with the analytical proof of stability for such a control architecture. Moreover, the stability analysis has been addressed also for the PD controller.

The testbed setup consists of a master-slave system composed by an Omega Haptic Device (master) and a KUKA KR3 robot (slave). We qualitatively evaluated the system performance in three telemanipulation tasks: rigid contact with high stiffness objects, soft contact with a deformable object and finally the insertion of a needle into a soft ma-

*E-mail: {manganelli, chinello, formaglio, prattichizzo}@dii.unisi.it

terial. The results stemming from this preliminary study show that in spite of its simplicity, the task-oriented design better satisfies the requirements for the application of interest.
The remainder of this paper is structured as follows: in Section 2 we model the teleoperation system, the Section 3 discusses the adopted control strategies, the Section 4 reports experiments and results, and finally the Section 5 concludes this work.

2. The prototype system

The teleoperation system features a master-slave configuration. The master device is the Omega.3 haptic interface (ForceDimension). It is remotely handled by the operator to drive the endoscope insertion and it renders the interaction forces fed back by the controller.
As already mentioned in the introduction, the application of interest consists of safely driving a linear-stage endoscope into the brain of the patient. Since the brain tissues are very soft and feature a jelly-like dynamical behavior, the insertion is a high-risk task the contact forces measured by the endoscopic probe during the penetration are very small. In order to improve the safety and the precision, the master measured motion is scaled, using a constant factor to smooth the reference input signal for the slave robot. Also, the forces experienced by the end-effector linear stage are amplified before being rendered to the surgeon's hand by the master haptic interface.
The insertion task features a single translational degree of freedom (DoF). To that end, we mechanically customized the Omega in order to constrain the possible motion along only a single DoF, as shown in Fig. 1 (left). In addition, the end-effector has been replaced with a stylus. The slave device is the anthropomorphic manipulator KUKA KR3

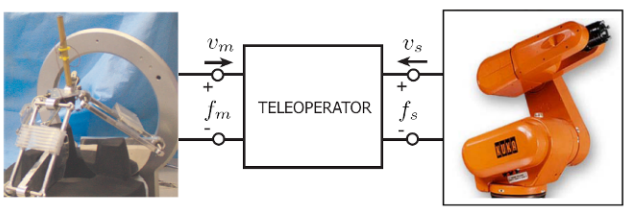

Figure 1. *The teleoperator setup. Left: the master device. Center: the two-port interconnection architecture. Right: the slave linear actuator.*

reported in Fig. 1 (right). Table 1 reports the main technical specifications of the slave robot. As for the master robot, the slave is also constrained along a single DoF to run the experiment. The KR3 robot

Table 1. *Technical specifications of the KR3 manipulator.*

Kinematics	anthropomorphic - 6 DoF
Workspace	Max reach 650mm
3D Resolution	0.001mm
Repeatability	$< \pm 0,02$mm
Peak Force	35N
Max Velocity	5m/sec

is a discrete-time system featuring sampling time $T_s = 12$ ms, its end-effector motion can be controlled by applying force or velocity reference signals, defined in the joint space or in the operational space.
In order to measure the forces due to the interaction with the environment, the slave end-effector was instrumented with a 1—DoF force sensor. The data acquisition setup, including the sensor power supply and a National Instrument 6014-PCI acquisition device, was tuned to measure forces ranging from -12 N to 12 N, with a resolution of 0.4 mN.

3. Control design

According to Passivity Control Theory [12], a master-slave teleoperator is stable if it is passive. In other terms, it should convey signals without increasing their energy. Modeling the system as a two-port electric network, the methods of electrical engineering can be easily used to evaluate the network energy and to check whether the control loop is passive or not. To that end, the teleoperator has been modeled as a two-port network (Fig. 2), where the master and slave forces f_m and f_s are the efforts, and the master and slave velocities v_m are the flows, (Fig. 1). The system inputs are $v_m(n)$ and $f_s(n)$, while the outputs are the $f_m(n)$ and $v_s(n)$. As mentioned above, the operator's commanded motion and the measured force can be scaled by user-defined factors k_v and k_f respectively, yielding $\bar{v}_m(n) = k_v v_m(n)$ and $\bar{f}_m(n) = k_f f_m(n)$. According to classic theory of electrical networks, the energy flow is computed for each port, and the amount of energy stored in the network is equal to the energy introduced through the master port minus the energy conveyed through the slave port. If the stored energy is negative, it means that the slave energy is greater than the master energy, i.e. the system is generating energy, it is not passive and the stability is no longer guaranteed. Hence, the passivity (and hence the stability) is guaranteed if the stored energy is non-negative.
The key idea of the Time-Domain Passivity Control consists of measuring the energy flows at the master and slave ports. If the system becomes active, the exceeding energy is dissipated by a Passivity Controller (PC) connected with each port.

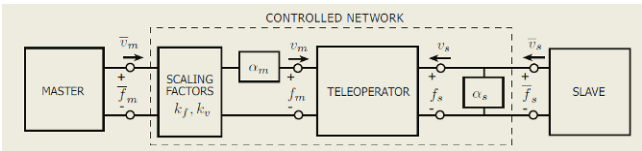

Figure 2. *The two-port control architecture.*

A Passivity Observer (PO) is employed to monitor the port energy at each time instant. The energy at the n^{th} time instant is computed as:

$$\begin{aligned} W(n) &= \overline{W}(n-1) + k_f k_v \Delta W_m(n) + \Delta W_s(n) \\ \overline{W}(n-1) &= \sum_{k=0}^{n-1} [\bar{f}_m(k)\bar{v}_m(k) + \bar{f}_s(k)\bar{v}_s(k)] \\ \Delta W_m(n) &= f_m(n) v_m(n) \\ \Delta W_s(n) &= f_s(n) v_s(n) \end{aligned} \tag{1}$$

The network is passive until $W(n) \geq 0$, otherwise the system stability is no longer guaranteed. The classic approach consists of activating

the PC only when $W(n) \geq 0$ [12]. Given the high risk level of our application, we adopted a more conservative strategy, which consists of activating the PC as soon as the current energy becomes smaller than the predefined threshold $W_0 = 2f_{max}v_{max}$, where f_{max} and v_{max} are the maximum force and velocity allowed by the system. In the worst case W_0 is the maximum energy output that can occur in one time step. This strategy guarantees that in the time instant the PC is activated, the energy is such that $0 < W(n) < W_0$. As it is shown in Fig. 2, we add one series PC $\alpha_m(n)$ to the master port and a parallel PC $\alpha_s(n)$ to the slave port, therefore the controlled network constitutive laws become:

Master PC:

$$\bar{v}_m(n) = k_v v_m(n)$$
$$\bar{f}_m(n) = k_f f_m(n) + \alpha_m(n) v_m(n)$$

if $W(n) \geq W_0$:

$$\alpha_m(n) = 0$$

otherwise:

$$\alpha_m(n) = \begin{cases} -k_f \frac{f_m(n)}{v_m(n)} & \Delta W_m(n) < 0 \text{ and } \Delta W_s(n) \leq 0 \\ -k_f \frac{f_m(n)}{v_m(n)} - \frac{\Delta W_s(n)}{k_v v_m^2(n)} & \Delta W_m(n) < 0 \text{ and } \Delta W_s(n) > 0 \\ 0 & \Delta W_m(n) \geq 0 \end{cases} \tag{2}$$

Slave PC:

$$\bar{f}_s(n) = f_s(n)$$
$$\bar{v}_s(n) = v_s(n) + \frac{1}{\alpha_s(n)} f_s(n)$$

if $W(n) \geq W_0$:

$$\alpha_s(n) = \infty$$

otherwise:

$$\alpha_s(n) = \begin{cases} -\frac{f_s(n)}{v_s(n)} & \Delta W_s(n) < 0 \text{ and } \Delta W_m(n) \leq 0 \\ \left(-\frac{v_s(n)}{f_s(n)} - k_f k_v \frac{\Delta W_m(n)}{f_s^2(n)} \right)^{-1} & \Delta W_s(n) < 0 \text{ and } \Delta W_m(n) > 0 \\ \infty & \Delta W_s(n) \geq 0 \end{cases} \tag{3}$$

It can be easily demonstrated that using the master and slave controllers (2) and (3) the system passivity is always guaranteed:

$$\begin{aligned} \overline{W}(n) &= \sum_{k=0}^{n} [\bar{f}_m(k)\bar{v}_m(k) + \bar{f}_s(k)\bar{v}_s(k)] \\ &= \sum_{k=0}^{n-1} [\bar{f}_m(k)\bar{v}_m(k) + \bar{f}_s(k)\bar{v}_s(k)] + \bar{f}_m(n)\bar{v}_m(n) + \bar{f}_s(n)\bar{v}_s(n) \\ &= \overline{W}(n-1) + k_f k_v f_m(n) v_m(n) + f_s(n) v_s(n) \\ &\quad + k_v \alpha_m(n) v_m^2(n) + \frac{1}{\alpha_s(n)} f_s^2(n) \\ &= \overline{W}(n-1) \end{aligned} \tag{4}$$

Hence, using equations (2) and (3), the energy stored in the controlled network is $\overline{W}(n) > 0 \ \ \forall\, n$, hence the stability is ensured in any condition.

The energy evaluation and the eventual dissipation is based on the measured signals, hence it is crucial to have reliable measurements and to filter out the noise without introducing the phase delay usually caused by low-pass filtering. To that end, the discrete-time First Order Adaptive Windowing (FOAW) filter introduced in [14] has been implemented to smooth the commanded velocity signal. It originates from common FIR filters, but the time window size is set as the maximum size such that the straight line joining the extreme samples passes through the uncertainty interval of each sample falling inside the window. Hence, as the size h is adapted, the velocity sample $\hat{v}(n)$ at time instant n is computed as:

$$\hat{v}(n) = \frac{1}{h T_c}(x(n) - x(n-h)) \tag{5}$$

where $x(n)$ is the end-effector position at time instant n, and T_c is the sample time (for more details about the FOAW filter, please refer to [14]). Smoothing the insertion velocities will result in measuring smoother contact forces at the endoscope tip, reducing the noise in the force feedback profile rendered to the surgeon's hand.
The main drawback of this technique is that the control effort determined by the PC can lead to actuator saturation. Generally, in order to prevent saturation, the PC signal is upper bounded, but this in turn can result in a drop in performance. In fact, in such a case the dissipation of the exceeding energy may require more than one time step, leading to transient vibration effects.
A simpler control strategy has been designed for this teleoperation system relying on the assumption that the user's commanded motions during microinvasive neurosurgery interventions will be slow and sharp, thus also the force reflection will be fed back with slow dynamics. Hence, we designed a simple proportional-derivative (PD) controller in order for the slave end-effector to track the master end-effector motion, filtering out all frequency contents exceeding a predefined bandwidth. Hence, the PD transfer function $C(s)$ is defined as:

$$C(s) = k_P + s k_D \tag{6}$$

The block scheme for the teleoperation system can be simply represented as:

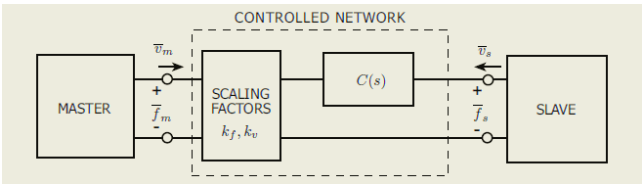

Figure 3. The master-slave teleoperator system with the PD controller.

The slave device has been simply modeled as an integrator, yielding the transfer function $\frac{1}{s}$. The proportional and derivative factors have been designed using classical control theory [15], according to the desired closed-loop performance. As regards stability, we chose again the approach of passivity. A system composed by passive subsystems is passive as well [12]. In the literature, the human model and the Omega Haptic Device have been demonstrated to be passive [16, 17], hence only the passivity of the controlled slave transfer function must be studied [18]. The PD parameters we tuned according to closed-loop performance specifications resulted as passive.
Again, the FOAW filter was adopted in order to filter out the noise from the velocity signals.

In addition to the effects of the control law, the haptic transparency of the teleoperator can also be affected by the gravitational force. While using the master device, the mass perceived by the surgeon at the haptic handle is due to gravity acting on the whole mechanical structure of the master device. Compensating these effects of gravity is not straightforward, since generally they depend on the end-effector position in the workspace through a non-linear relationship. We adopted the Autocalibrated Gravity Compensation technique [19]. The strategy consists of performing an off-line recursive estimation of the apparent gravity force acting at a certain set of positions inside the workspace. Secondly, the on-line gravity compensation at an arbitrary position is computed by interpolating the estimated data. The stability of the Autocalibrated Gravity Compensation has been analytically proved in [20]. The compensation algorithm has been adopted with both the PC and the PD controller. Anyway, we remark that this control stage is applied directly to the master device low-level control, it is not correlated with the control signals involved in the teleoperator, hence it has not been included in the two-port network.

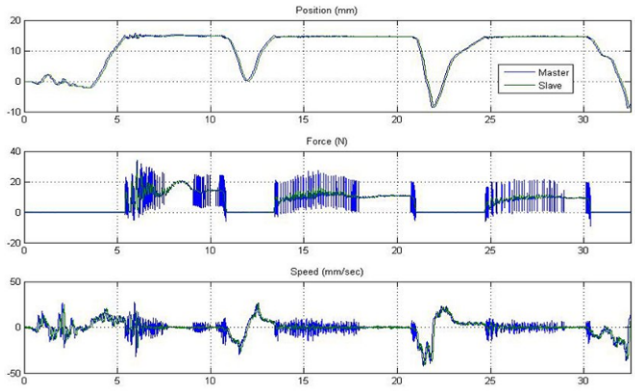

Figure 5. *Trajectories for a rigid contact using PC control.*

4. Experiments

Several experiments have been carried out to evaluate the performance of the teleoperation system using passivity control (PC) and low-pass proportional-derivative (PD) control. The threshold energy for the PC was $W_0 = 120J$, stemming from $f_{max} = 12N$ and $v_{max} = 0.005m/s$, while the PD parameters were $k_P = 3$ and $k_D = 0.35$, designed according to the model of the KR3. In the following, we report the results achieved in three teleoperation tasks: rigid contact, soft contact and needle insertion. For each task, we recorded position, velocity and force of both master and slave end-effectors.

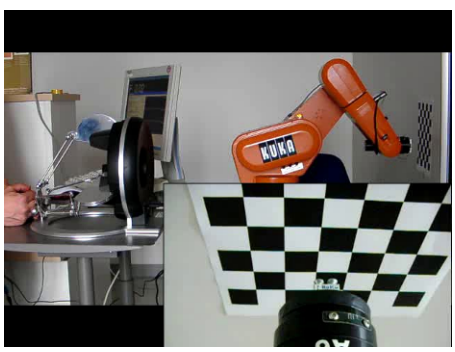

Figure 4. *First task: rigid contact with a high stiffness object.*

In the first task, the contact with a rigid wall was performed, as shown in Fig. 4. The experimental data acquired using PC control and PD control are shown in Fig. 5 and Fig. 6 respectively. The second task consisted in remotely touching the foam rubber dice depicted in Fig. 7, whose stiffness has been estimated as approximately $100\frac{N}{m}$. Figs. 8 and 9 show the data recorded during the contact, using PC control and PD control.

Finally, the third task consisted in remotely inserting a syringe needle into an organic material. To this end, the needle was rigidly attached to the slave end-effector, as shown in Fig. 10. We were interested in experiencing the effects of penetration and of viscous dumping due to the perforation of the skin and of the internal pulp. In this experiment,

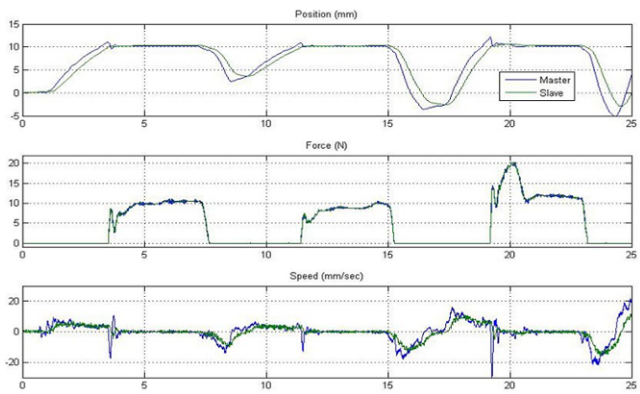

Figure 6. *Trajectories for a rigid contact using PD control.*

as a target object we chose a kiwi fruit. As expected, the forces stemming from this type of interaction were very difficult to be perceived by the user, hence it was necessary to amplify the measured forces. Fig. 11 and Fig. 12 show the trajectories recorded during the contact, using PC control and PD control, and amplifying the forces with a gain $k_f = 10$. The PC was able to restore the system passivity every time it was required during all tasks, thus guaranteeing the system stability. Using the PD controller, the system was always stable. In terms of master-slave position tracking, in the case of rigid contact the PC performance was slightly higher than that of PD, while in the other tasks there were no significant differences. On the other hand, considering the haptic feedback, the PD was always able to render smooth contact forces, while the PC generally delivered noisy force profiles. This can be ascribed to the PC efforts required to restore the system passivity. Recall that as soon as the passivity observer reveals that the energy is lower than the threshold, the controller attempts to instantly dissipate the energy flow from each active port in a single step. Hence the PC impulsive control efforts can affect the haptic feedback, providing a noisy force profile.

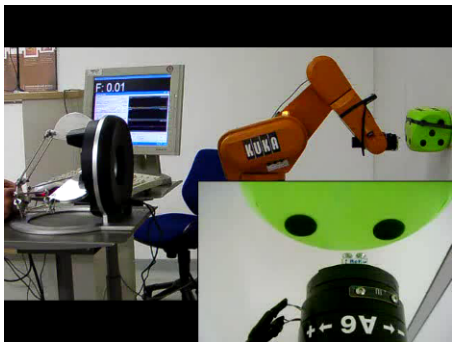

Figure 7. *Second task: soft contact with a deformable object.*

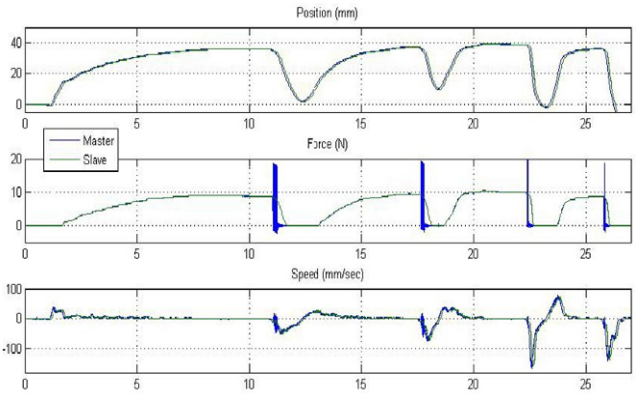

Figure 8. *Trajectories for a soft contact using PC control.*

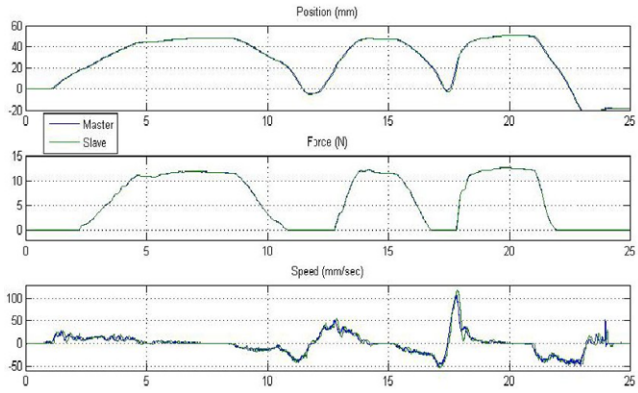

Figure 9. *Trajectories for a soft contact using PD control.*

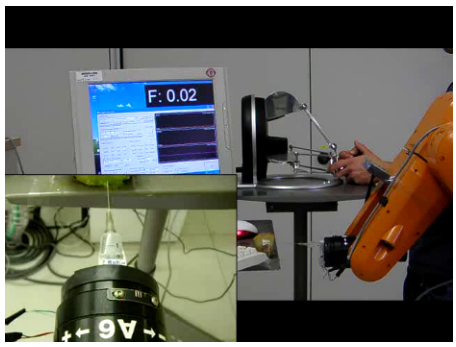

Figure 10. *Third task: insertion of a needle into a soft material simulated by a kiwi fruit.*

5. Conclusion

This paper addresses design issues characterizing a teleoperation control system targeted at driving the insertion of a linear-stage rigid endoscope into the brain of a patient for neurosurgery interventions. We present preliminary results of our current research, addressed towards evaluating the applicability of a general-purpose control scheme compared to a specific and task-oriented architecture.

The general-purpose control scheme we chose was the time-domain passivity control. Meanwhile, the task-oriented scheme was a proportional-derivative control, based on the assumption that during microsurgery interventions the user's commanded motions and the reflected forces will be characterized by slow dynamics. Hence, the PD was designed in order to filter out all surgeons motions exceeding a predefined bandwidth, thus privileging task accuracy and safety in spite of a loss of dynamical performance.

The experimental setup was a master-slave system composed by a Omega Haptic Device (master) and a KUKA KR3 robot (slave). Three tasks were performed to qualitatively evaluate the system performance: rigid contact with high stiffness objects, soft contact with a deformable object and finally the insertion of a needle into a perforable material. The results stemming from this preliminary study show that even if the task-oriented design provides lower dynamical performance than the

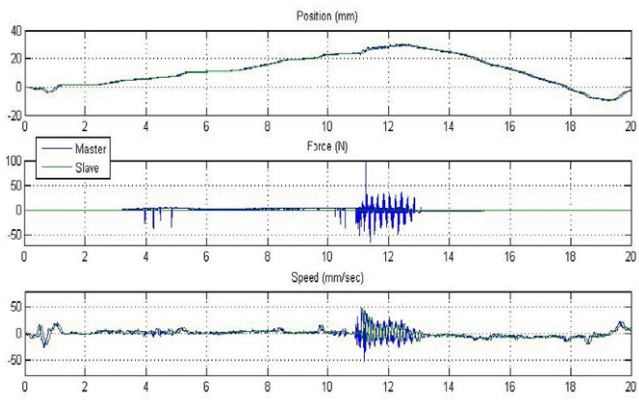

Figure 11. *Trajectories for needle insertion using PC control, with a force gain* $k_f = 10$.

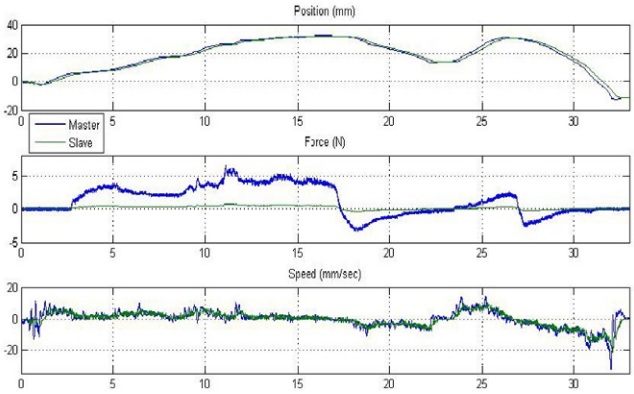

Figure 12. *Trajectories for needle insertion using PD control, with a force gain* $k_f = 10$.

general-purpose one, it revealed to be stable and was able to render smoother forces in any situation, improving the user's kinesthetic perception during the task remote control.

Acknowledgments

This work is supported by the European Commission under CP grant FP7-ICT-2007-215190 "ROBOCAST: ROBOt and sensors integration for Computer Assisted Surgery and Therapy", and under CP grant FP7-ICT-2009-6-270460 "ACTIVE: Active Constraints Technologies for Ill-defined or Volatile Environments".

References

[1] P.F. Hokayem and M.W. Spong. Bilateral teleoperation: An historical survey. Automatica, 42(12):2035-2057, 2006.

[2] RoboCAST: ROBOt and sensors integration for Computer Assisted Surgery and Therapy - Grant FP7-ICT-2007-215190 - http://www.robocast.eu/.

[3] Y. Yokokohji and T. Yoshikawa. Bilateral control of master-slave manipulators for ideal kinesthetic coupling-formulation and experiment. IEEE transactions on robotics and automation: a publication of the IEEE Robotics and Automation Society, 10(5):605, 1994.

[4] D.A. Lawrence. Stability and transparency in bilateral teleoperation. IEEE Transactions on Robotics and Automation, 9(5):624-637, 1993.

[5] M.C. Çavusoglu, A. Sherman, and F. Tendick. Design of bilateral teleoperation controllers for haptic exploration and telemanipulation of soft environments. IEEE Transactions on Robotics and Automation, 18(4):641-647, 2002.

[6] JE Colgate. Robust impedance shaping telemanipulation. IEEE transactions on Robotics and Automation, 9(4):374-384, 1993.

[7] B. Hannaford. A design framework for teleoperators with kinesthetic feedback. IEEE transactions on Robotics and Automation, 5(4):426-434, 1989.

[8] J.H. Ryu and D.S. Kwon. A novel adaptive bilateral control scheme using similar closed-loop dynamic characteristics of master/slave manipulators. Journal of Robotic Systems, 18(9):533-543, 2001.

[9] R.J. Anderson and M.W. Spong. Asymptotic stability for force reflecting teleoperators with time delay. The International Journal of Robotics Research, 11(2):135, 1992.

[10] S.E. Salcudean. Control for teleoperation and haptic interfaces. Lecture Notes in Control and Information Sciences, pages 51-66, 1998.

[11] T. Haidegger, L. Kovacs, S. Preitl, R.E. Precup, B. Benyo, and Z. Benyo. Controller Design Solutions for Long Distance Telesurgical Applications. International Journal of Artificial Intelligence, 6(S11):48-71, 2011.

[12] J.H. Ryu, D.S. Kwon, and B. Hannaford. Stable teleoperation with time-domain passivity control. IEEE Transactions on robotics and automation, 20(2):365-373, 2004.

[13] J. Semmoloni, R. Manganelli, A. Formaglio, and D. Prattichizzo. Control design issues for a microinvasive neurosurgery teleoperator system. In Advanced Robotics, 2009. ICAR 2009. International Conference on, pages 1-5. IEEE, 2009.

[14] F. Janabi-Sharifi, V. Hayward, and C.S.J. Chen. Discrete-time adaptive windowing for velocity estimation. Control Systems Technology, IEEE Transactions on, 8(6):1003-1009, 2000.

[15] S.P. Boyd and C.H. Barratt. Linear Controller Design: Limits of Performance. Prentice Hall, 1991.

[16] J.E. Colgate, M.C. Stanley, and J.M. Brown. Issues in the haptic display of tool use. In Intelligent Robots and Systems 95.'Human Robot Interaction and Cooperative Robots', Proceedings. 1995 IEEE/RSJ International Conference on, volume 3, pages 140-145. IEEE, 2002.

[17] J.E. Colgate and G. Schenkel. Passivity of a class of sampled-data systems: Application to haptic interfaces. In American Control Conference, 1994, volume 3, pages 3236-3240. IEEE, 2002.

[18] R. Lozano, B. Brogliato, O. Egeland, and B. Maschke. Dissipative Systems Analysis and Control. Theory and Applications. Measurement Science and Technology, 12:2211, 2001.

[19] A. Formaglio, M. Fei, S. Mulatto, M. de Pascale, and D. Prattichizzo. Autocalibrated gravity compensation for 3 DoF impedance haptic devices. 5024:43-52, June 2008.

[20] A. Formaglio, S. Mulatto, and D. Prattichizzo. Iterative estimation of the end-effector apparent gravity force for 3dof impedance haptic devices. In Proc. EUCA European Conference on Control, Budapest, Hungary, August 2009.